



Development of Volcano Warning System for Kelud Volcano

Maria Evita¹, Azka Zakiyyatuddin¹, Sensius Seno¹, Nina Siti Aminah¹, Wahyu Srigutomo¹, Irwan Meilano², Ari Setiawan³, Herlan Darmawan³, Imam Suyanto³, Irzaman⁴, Mohammad Yasin⁵, Perdinan⁶, Retna Apsari⁵, Wahyudi³, Wiwit Suryanto³ & Mitra Djamal^{1,7,*}

¹Department of Physics, Faculty of Mathematics and Natural Sciences, Institut Teknologi Bandung, Jalan Ganesa No. 10, Bandung 40132, Indonesia

²Faculty of Earth Sciences and Technology, Institut Teknologi Bandung, Jalan Ganesa No. 10, Bandung 40132, Indonesia

³Department of Physics, Faculty of Mathematics and Natural Sciences, Universitas Gajah Mada, Sekip Utara, Bulak Sumur, Yogyakarta 55281, Indonesia

⁴Department of Physics, Faculty of Mathematics and Natural Sciences, Jalan Meranti Gedung Wing S No. 3, Dramaga, Bogor 16680, Institut Pertanian Bogor, Indonesia

⁵Department of Physics, Faculty of Science and Technology, Universitas Airlangga, Jalan Mulyorejo, Surabaya 60115, Indonesia

⁶Department of Geophysics and Meteorology, Faculty of Mathematics and Natural Sciences, Jalan Meranti Gedung Wing S No. 3, Dramaga, Bogor 16680, Institut Pertanian Bogor, Indonesia

⁷Department of Physics, Faculty of Sciences, Institut Teknologi Sumatera, Jalan Terusan Ryacudu, Way Hui, Jati Agung, Lampung Selatan 35365, Indonesia

*E-mail: mitra@fi.itb.ac.id

Highlights:

- A volcano warning system based on the Internet of Things, using sensors, a drone, a mobile robot, and satellite imagery was developed and applied for Mount Kelud, Indonesia.
- The warning system was developed using fuzzy logic.
- The measured parameters were seismicity, gas concentrations and temperature.

Abstract. Kelud is a volcano in Indonesia located between the Kediri and Blitar districts of East Java province. This volcano has erupted multiple times between the year 1000 and 2014, resulting in over 200,000 casualties. Therefore, a volcano warning system is needed to detect forthcoming eruptions to minimize the number of casualties. A warning system was developed based on sensor nodes comprising vibration, temperature and gas (sulfur and carbon dioxide) sensors to monitor physical parameters of the volcano, drone surveillance, mapping and temperature measurement, and a mobile robot carrying the same sensors as the sensor nodes for both normal and emergency situations. The system was tested on the Kelud volcano in normal condition in August 2019. The system detected 1 Hz of seismicity, under 1 ppm of sulfur and carbon dioxide, lake temperature at 23 °C to

55.3 °C, ground temperature at 32 °C, and air temperature between 23 °C and 25 °C. The system can be used for 37 hours at full operation with 1 charging cycle of the solar cell and is suitable for application in a dangerous environment.

Keywords: *drones; warning system; fuzzy control; gas, Kelud; mobile robots; seismicity; sensors; temperature; volcano.*

1 Introduction

Indonesia lies within the Ring of Fire of Asia Pacific volcanoes and has 129 active volcanoes. As an andesitic small stratovolcano, Mount Kelud is one of the most active and often destructive volcanos in Indonesia [1-7]. It not only has hazardous explosive eruptions but also short effusive eruptions, where lava, lahars, pyroclastic and acid magma with high gas concentrations form an edifice [3,4]. This volcano is located at 7°56'S and 112°18'E in East Java at 1731 m above sea level and 1650 m above populated areas in the Kediri and Blitar districts. After its first eruption in 1000 (the oldest known eruption in Indonesia), the largest eruptions took place in 1586, 1641, 1828, 1919, 1951, 1966, 1990 and 2014 [3,5,8]. The total number of casualties of these eruptions was more than 200,000 people from 35 villages surrounding the volcano, together with damage to livestock, buildings, infrastructure, agriculture, etc. [1,4,7,9]. The damage was caused by high energy released (2.2×10^9 J during the 2014 eruption and 3×10^8 J during the 2007 eruption) from the magma traveling at high velocity (over 200 m/s) in a plinian eruption [1,9].

The eruption usually begins with some seismic activity, followed by lava dome growth, volcano-tectonic and shallow volcanic (VB) earthquakes as a rock stress response to magmatic movement from tectonic activity and thermal conduction of magma chambers and an increase of earthquake events (more than 1400/day), finally leading to an eruption [1,3,4,10,11]. The seismic activity was preceded by an increase in the temperature of the crater lake, measured by temperature sensors about three months before the eruption, from ambient temperature (19 °C to 30 °C) to about 80 °C right before the eruption [5,8,12,13]. The heat resulted from a combination of hydrothermal-fluid, enthalpy-solar and atmospheric radiation [12]. The seismic activity was also preceded by a change in levels of CO₂ (30% in gaseous state) and SO₂ in the crater [3-5,9,12,14]. A few hours after the eruption, volcanic ash began to spread, reaching about 500 km westward from the volcano, as detected in satellite images [1,7]. Unfortunately, lava and lahars also caused the measurement system to break and for safety reasons no manual measurements were done, while the data could not be acquired afterwards [1,3,5]. Therefore, in this research we have developed a volcano warning system based on Internet of Things-sensor nodes comprising a vibration sensor for seismicity measurement, temperature, CO₂ and SO₂ sensors, drone surveillance, mapping

and temperature measurement, satellite image data for climate analysis of cloud ash erupting from the volcano, and a mobile robot equipped with the same sensors as the sensor nodes for both normal and emergency situations in case the system fails to send data or is broken because of an eruption.

2 Methodology

In this research, physical parameter data from the volcano, i.e. seismicity, temperature, gas concentrations (SO_2 and CO_2), are transmitted to a base station and then relayed to a center station for further processing and analysis combined with satellite image data. The sensor nodes being in a fixed location for initial monitoring is called fixed mode (pink arrows in Figure 1) [15-19]. The robot and drone being activated to acquire the same data is called mobile mode (blue arrows in Figure 1) [15-19].

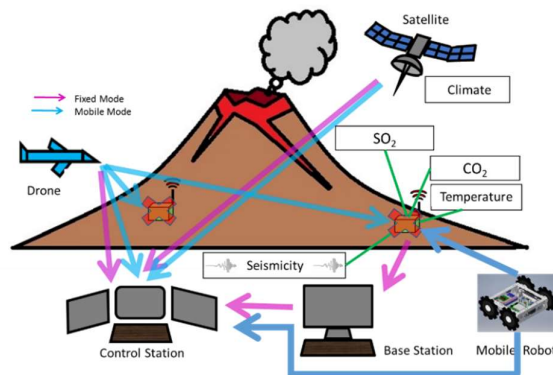


Figure 1 Volcano warning system.

The drone and the mobile robot are used in disaster conditions, when human safety (of the authorized officer) has higher priority than equipment safety [15-19]. These vehicles are deployed to the place where a broken sensor node is located. In this condition, the drone will acquire the data of the volcano 2 to 3 times a day for about 15 minutes (limited by its battery durability) for each data acquisition [20,21]. The robot will be deployed 2 to 3 times a day for data acquisition, which takes about 1 hour [22,23]. After acquiring the data, they both move to the location of another broken node. The satellite images are used to enrich the data analysis in emergency mode.

2.1 Smart Sensor System

The fixed-mode sensor nodes consist of a CO_2 sensor (MG811), a SO_2 sensor (TGS2602), a temperature and humidity sensor (DHT11), a seismicity sensor

(MPU6050), a microcontroller, a 12-watt on-board rechargeable solar cell battery for extended power supply durability, a long range radio (LoRa) for data transmission to the base station, a LoRa-WAN for data transmission from the base station to the center station. The real-time measurement data and fuzzy logic warning status can be accessed using the RED node of an Internet of Things module (Figure 2).

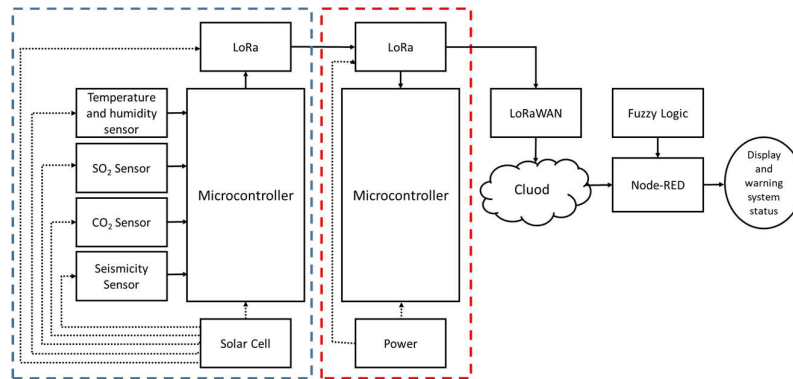


Figure 2 Smart sensor with microcontroller, LoRa for data transmission, sensors for temperature/humidity, SO₂, CO₂, and seismicity, solar cell and power with power supply line indicated by the dashed arrow, while the data flow is indicated by the solid arrow, both in the transmitter (blue dashed box) and the receiver (red dashed box).

In the fuzzification process, as the first step of fuzzy logic implementation [24], a triangle membership function is used to make the fuzzy rules that define the warning status of the volcano with four linguistic variables: *normal* (normal), *waspada* (caution), *siaga* (warning) and *awas* (evacuate) (Figure 3), as expressed in Eqs. (1)-(4).

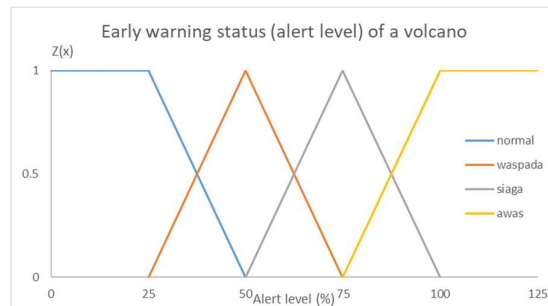


Figure 3 Triangle membership function for volcano warning status: *normal* (blue graph), *waspada* (orange graph), *siaga* (grey graph) and *awas* (yellow graph).

$$Z(x)_{Normal} = \begin{cases} 0, & x < 0 \\ 1, & 0 \leq x \leq 25 \\ \frac{50-x}{25}, & 25 \leq x \leq 50 \\ 0, & x \geq 50 \end{cases} \quad (1)$$

$$Z(x)_{waspada} = \begin{cases} 0, & x \leq 25 \\ \frac{x-25}{25}, & 25 \leq x \leq 50 \\ \frac{75-x}{25}, & 50 \leq x \leq 75 \\ 0, & x \geq 75 \end{cases} \quad (2)$$

$$Z(x)_{siaga} = \begin{cases} 0, & x \leq 50 \\ \frac{x-50}{25}, & 50 \leq x \leq 75 \\ \frac{75-x}{25}, & 75 \leq x \leq 100 \\ 0, & x \geq 100 \end{cases} \quad (3)$$

$$Z(x)_{awas} = \begin{cases} 0, & x \leq 75 \\ \frac{x-75}{25}, & 75 \leq x \leq 100 \\ 1, & x \geq 100 \end{cases} \quad (4)$$

where $Z(x)$ is the membership degree of each linguistic alert level variable and x is the alert level of each parameter. The alert levels of seismicity are categorized by the type of earthquake detected by the sensor nodes [25]. For example, a low-frequency (1-2 Hz), shallow and short-duration earthquake is categorized as 'normal'. Meanwhile, the levels of temperature are categorized by the air temperature detected by the sensors [26]. For example, the temperature range for the 'normal' level is under 37 °C. Furthermore, the gas alert levels are categorized by their effect on the human body as indicated by the concentrations detected by the sensors [27,28]. For example, the 'normal' level is under 12 ppm and 600 ppm for the SO₂ and the CO₂ concentration respectively. The combination possibilities of the four sensors (SO₂, CO₂, temperature and seismicity) form 53 fuzzy rules for the alert levels. For example, if SO₂ is 'normal', CO₂ is 'normal', temperature is 'normal' and seismicity is 'normal', then the warning status is also 'normal'.

The clipping inference process of the fuzzy logic uses the Mamdani model, because of its easy implementation. It has to be defuzzified by composition when it is aggregated with other functions to form a singular fuzzy set [29]. The inference uses a conjunction for the minimum membership degree of the linguistic variables:

$$\text{Conjunction: } T(P \wedge Q) = \min\{T(P), T(Q)\} \quad (5)$$

where P is between $[0,1]$ and T is the ‘true’ function of P to interval $[0,1]$.

The last step in fuzzy logic is defuzzification [30]. The weighted average method is used to generate the crisp value:

$$y^* = \sum \frac{\mu(y)y}{\mu(y)} \quad (6)$$

where y is the crisp value and $\mu(y)$ is the membership degree of crisp value y . These values are then substituted by the linguistic variables of the volcano warning system and alert level curves can be plotted using Eqs. (1)-(4).

2.2 LoRa and LoRaWAN

LoRa is a frequency modulation format using phase shift keying (PSK) and frequency shift keying (FSK) transmission with a stable frequency value [31]. This low-cost (both in terms of purchase and power consumption) radio can be implemented for long-range applications until 100 km with high capacity and security (using end-to-end AES128 encryption), and also for geolocation [32]. In this research, this M2M (machine-to-machine) communication method was used for the transducers of the transmitter and the receiver.

LoRaWAN uses a star-on-star topology (for efficient power consumption and an increased communication range, especially for the tracking devices) to transmit messages to the center server through a gateway for collision avoidance. This transmission process provides redundancy detection, security detection, scheduling and message transmission. LoRaWAN has been tested over 4.3 km of urban area and 9.7 km of open village space [33], therefore it was suitable to be applied in this research for real-time high-resolution data communication.

2.3 Solar Cell and Battery

A renewable energy source was used for the power supply in this research, employing a solar cell, which is suitable for Indonesia with all-year sunshine. The harvested electric energy was stored in a battery as chemical energy.

$$\text{Solar cell current} = \frac{\text{Solar cell power}}{\text{Solar cell voltage}} \quad (7)$$

The current consumed by the system and its lifetime are formulated in Eq. (8) and (9):

$$\text{Current}_{\text{consumption}} (\text{ampere}) \cong \frac{\text{Power consumption (watt)}}{\text{Voltage of battery (volt)}} \quad (8)$$

$$\text{Battery lifetime} = \frac{\text{ampere hou of battery (ampere hour)}}{\text{current}_{\text{consumption}} (\text{ampere})} \quad (9)$$

The battery should be charged when it is empty, therefore the maximum current capacity of the battery should be known for calculating the charging time.

$$\text{Charging time (h)} = \frac{\text{Battery ampere hour (ampere hour)}}{\text{Solar cell current (ampere)}} \quad (10)$$

2.4 Drone

A quadcopter equipped with a Gimbal 12 MP camera and a 5870 mAh drone battery from DJI was used for this research. This Phantom 4 Pro series drone was controlled using the Phantom 4 Pro software on a smartphone along with the DJI GO application. After images have been taken by the drone, which flies following a flight plan, they are exported to the software to build a 3D model and an orthophoto for further analysis [20,21].

2.5 Mobile Robot

A robot with a proportional-integral-derivative (PID) controller using a skid-steering mechanism, Robot Operating System (ROS), Real Time Operating System (RTOS) for kinematics and dynamics was used to acquire volcano parameter data (SO₂ CO₂, temperature and seismicity) while in mobile mode [22,23].

3 Result and Discussion

3.1 Seismicity

Raw data in the form of acceleration versus time were computed using the fast Fourier transform (FFT) for frequency domain transformation. Hereafter they are presented as their root mean square (RMS) value (Figure 4), after calculating the power spectral density (PSD). Thus, the spectral component contribution for each frequency can be analyzed [34].

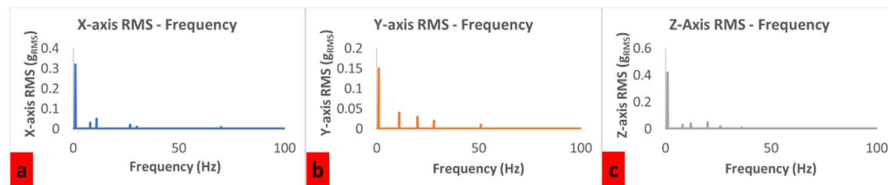


Figure 4 The x-axis RMS until a frequency of 100 Hz (a), the y-axis RMS (b) and the z-axis RMS (c) for Mount Kelud in August 2019.

Moreover, it can be seen that the seismicity was only 1 Hz for 0.32 g_{RMS} on the x-axis, 0.15 g_{RMS} on the y-axis and 0.42 g_{RMS} on the z-axis (Figure 4), which can

be categorized as a normal level for this volcano. The other peaks in Figure 4 can be considered noise from the device, with low-frequency noise (until 10 Hz) about 0.03 g_{RMS} and 0.05 g_{RMS} up to 100 Hz [35].

3.2 Gas Concentrations

The sulfur dioxide concentration slightly varied between 0.298 and 0.464 ppm, similar to the carbon dioxide concentration, which varied from 0.306 to 0.391 ppm (Figure 5). According to the datasheet these ranges are categorized as noise, where the typical detection range is 1 to 10 ppm for SO₂ [36] and 300 to 10,000 ppm for CO₂ [37]. Therefore, there no contaminant gases were measured during this observation and the volcano was in normal condition. In the future, more data processing using a suitable filter will be done before the data are presented for analysis.

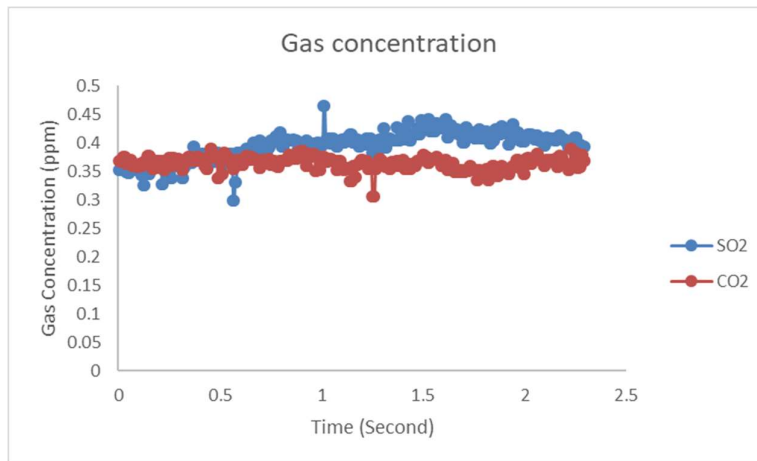


Figure 5 Sulfur dioxide concentration (blue graph) and carbon dioxide concentration (orange graph) of for Mount Kelud in August 2019.

3.3 Temperature

It can be seen from the map in Figure 8 that the temperature of the crater lake varied between 29.5 °C and 55.3 °C (Figure 6), while the ground temperature was 32 °C and the air temperature was between 23 °C and 25 °C at around 12 a.m. (inset of Figure 7), which can be categorized as a normal condition for this volcano. The temperature data were confirmed by other devices: a thermos-gun for the ground temperature (red graph of Figure 10) and Automatic Weather System (AWS) for the air temperature (blue graph of Figure 7).

Development of Volcano Warning System for Kelud Volcano

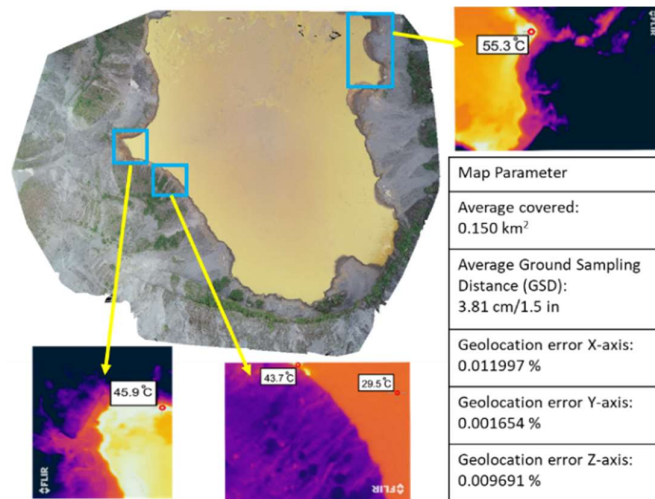


Figure 6 Temperature of the crater of Mount Kelud in August 2019 using an infrared sensor of the drone and a parameter map (top left) constructed from drone images (inset table).

From the inset table in Figure 6 it can be concluded that the map had a geolocation error (difference between initial and computed images) of about 0.01% for the x, y and z axis for 0.15 km² of average covered and an average ground sample distance (GSD) of 3.81 cm/1.5 in. This error is sufficiently small for the construction of a map of the Kelud crater from drone images [20,21].

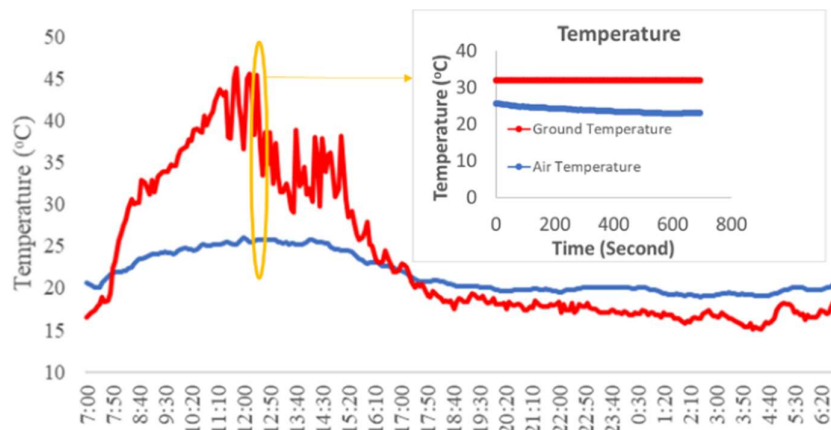


Figure 7 Ground temperature (red graph) and air temperature (blue graph) of the Kelud volcano in August 2019 from 7 a.m. to 7 a.m. the next day and temperature (ground and air) of Mount Kelud at around 12 a.m. (inset graph).

3.4 Volcano Warning Status

Based on the field data for SO₂ (0.298 to 0.404 ppm), CO₂ (0.306 to 0.191 ppm), air temperature (23 °C to 25 °C) and seismicity (1 Hz) as fuzzy input data for the fuzzification process, SO₂ was at a normal level [27], CO₂ was at a normal level [28], seismicity and air temperature were also at a normal level [25,26]. Only one fuzzy rule was used for this condition from the membership function of the graph in Figure 3: IF SO₂ = normal AND CO₂ = normal AND TEMPERATURE = normal AND SEISMICITY = normal THEN WARNING = NORMAL. Therefore, the clipping inference process (Eq.(5)): IF SO₂ = normal (≈ 0) AND CO₂ = normal (≈ 0) AND TEMPERATURE = normal (≈ 0) AND SEISMICITY = normal (≈ 0) THEN WARNING = NORMAL (≈ 0). The membership degree value of the defuzzification process used $Z(x)_{\text{normal}} = 0$ (Eq. (1)), $\frac{50-x}{25} = 0$. Moreover, the level value (x) of this condition, $x = 50\%$. Therefore, the alert level value for the Kelud volcano from these field data according to (Eq. 6) was $y = 0 \times 50 = 0\%$ (NORMAL).

3.5 Solar Cell and Battery

Generally, the data were acquired between 11 and 12 am. For this time range the output power of the solar cell is presented in Figure 8, where the average power was 10.88 watt, the average voltage was 19.34 volt and the average current was 562.3 mA (Eq. (7)).

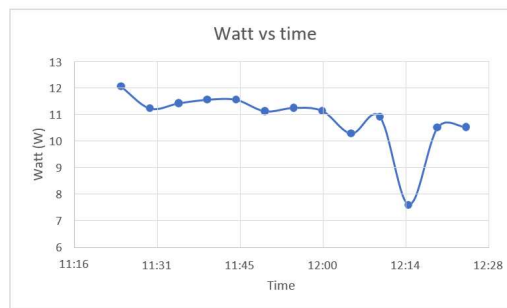


Figure 8 Output power of the solar cell over time.

The solar cell was designed to supply the power for the 12 volt/7 ampere/hour battery of the sensor system, which consumed about 2 watts of power in full operation mode (sensors, microcontroller, LoRa and other components). Therefore, the consumption current of the system was about 0.19 A (Eq. (8)). The battery was empty after about 37 hours in full operation mode (Eq. (9)). It could be recharged by the solar cell in about 12 hours of fully charging (Eq. (10)).

3.6 LoRa and LoRaWAN

In this research, we placed the sensor node and control station 400 m apart. Within this distance, the data could be received with a percentage error rate (PER) of only about 3%. However, when monitoring the volcano the distance will be greater, i.e. about 6 km as the distance from the summit to the observatory post on Mount Kelud.

4 Conclusion

A volcano warning system for Mount Kelud was developed. The system could detect a number of physical parameters of the volcano in normal condition, i.e. seismicity (1 Hz), gas concentrations (SO₂ and CO₂) under 1 ppm and temperature (23 °C to 55.3 °C for the lake, 32 °C for the ground and 23 °C to 25 °C for the air), which indicated that the system worked properly for about 37 hours in full operation mode until the battery had to be charged using the solar cell. However, the step of filtering the raw data is still needed before the data are presented for further analysis. In addition, a more powerful antenna should be used in the future for better data communication.

Acknowledgement

The authors would like thank Indonesian Collaboration Research (Riset Kolaborasi Indonesia) 2019-2020 from Institut Teknologi Bandung, Universitas Gajah Mada, Institut Pertanian Bogor and Universitas Airlangga for funding this research.

References

- [1] Maeno, F., Nakada, S., Yoshimoto, M., Shimano, T., Hokanishi, N., Zaenuddin & A., Iguchi, M., *A Sequence of a Plinian Eruption Preceded by Dome Destruction at Kelud Volcano, Indonesia, on February 13, 2014, Revealed From Tephra Fallout and Pyroclastic Density Current Deposits*, Journal of Volcanology and Geothermal Research, **382**, pp. 24-41, 2019.
- [2] Goode, L.R., Handley, H.K., Cronin, S.J. & Abrurrachman, M., *Insight into Eruption Dynamics From the 2014 Pyroclastic Deposits of Kelut Volcano, Java, Indonesia, and Implications for Further Hazards*, Journal of Volcanology and Geothermal Research, **382**, pp. 6-23, 2019.
- [3] Hidayati, S., Triastuty, H., Mulyana, I., Adi, S., Ishihara, K., Basuki, A., Kuswandarto, H., Priyanto, B. & Solikhin, A., *Differences in the Seismicity Preceding the 2007 and 2014 Eruptions of Kelud Volcano, Indonesia*, Volcanology and Geothermal Research, **382**, pp. 50-67, 2019.

- [4] Humaida, H., Brotopuspito, K.S., Pranowo, H.D. & Narsito, *Modelling of Magma Density and Viscosity Changes and Their Influences towards the Characteristics of Kelud Volcano Eruption*, Jurnal Geologi Indonesia, **6**(4), pp. 227-237, Dec. 2011. (Text in Indonesian and Abstract in English)
- [5] Hidayati, S., Basuki, A., Kristianto & Mulyana, I., *Emergence of Lava Dome from the Crater Lake of Kelud Volcano, East Java*, Jurnal Geologi Indonesia, **4**(4), pp. 229-238, Dec. 2009.
- [6] Wundermann, R. (ed.), *Report on Kelut (Indonesia)*, Global Volcanism Program, Bulletin of the Global Volcanism Network, **39**(2), Smithsonian Institution, Feb. 2014. DOI: 10.5479/si.GVP.BGVN201402-263280.
- [7] Lestiani, D.D., Apriyani, R., Lestari, L., Santoso, M., Hadisantoso, E.P. & Kurniawati, S., *Characteristics of Trace Elements in Volcanic Ash of Kelud Eruption in East Java, Indonesia*, Indones. J. Chem., **18**(3), pp. 457-463, 2018.
- [8] Bernard, A., *Kelud Volcano*, IAVCI Commission of Volcanic Lakes, www2.ulb.aac.be/science/cvl/DKIPART2.pdf (31 January 2020).
- [9] Nakamichi, H., Iguchi, M., Triastuty, H., Hendrasto, M. & Mulyana, I., *Differences of Precursory Seismic Energy Release for the 2007 Effusive Dome-forming and 2014 Plinian Eruption at Kelud Volcano, Indonesia*, Journal of Volcanology and Geothermal Research, **382**, pp. 68-80, 2019.
- [10] Lubis, A.M., *Uplift of Kelud Volcano Prior to the November 2007 Eruption as Observed by L-Band InSAR*, J. Eng. Technol. Sci., **46**(3), pp. 245-257, 2014.
- [11] Destawan, R., Bernando, A., Aziz, M. & Palupi, I.R., *Application of Tomography Seismic for Subsurface Modelling of Kelud Mountain*, AIP Conference Proceedings, **1730**, 2016.
- [12] Bernard, A. & Mazot, A., *Geochemical evolution of the young crater lake of Kelud volcano in Indonesia*, Water-Rock interaction (WRI-11), Wanty & Seal II, eds., A.A. Balkema Publishers, 2004.
- [13] Noor, A.B.S., Hidayat, R. & Perdinan, *The Analysis of Skin Surface Temperature and Water Vapor on Volcano Eruption (Case Study: Mt. Kelud)*, IOP Conference Series of the IsenREM 2019, **399**, 2019.
- [14] Caudron, C., Mazot, A. & Bernard, A., *Carbon Dioxide Dynamics in Kelud Volcanic Lake*, Journal of Geophysics Research, **117**, pp. B05102, 2012.
- [15] Djamal, M., Evita, M., Zimanowski, B & Schilling, K., *Development of Volcano Early Warning System*, Proceeding of Seminar Nasional Fisika 2015, Keynote Paper, 2015.
- [16] Djamal, M., Evita, M., Zimanowski, B. & Schilling, K., *Development of a Low-cost Mobile Volcano Early Warning System*, J. Tech. Sci., **1**(2), pp. 84-91, 2017.
- [17] Evita, M., Djamal, M., Zimanowski, B. & Schilling, K., *Mobile Monitoring System for Indonesian Volcano*, Proceeding of the 4th International

- Conference on Instrumentation, Communication, Information Technology, and Biomedical Engineering (ICICI-BME), pp. 278-281, 2015.
- [18] Evita, M., Djamal, M., Zimanowski, B. & Schilling, K., *Fixed-mode of Mobile Monitoring System for Indonesian Volcano*, Proceeding of the 4th International Conference on Instrumentation, Communication, Information Technology, and Biomedical Engineering (ICICI-BME), pp. 282-287, 2015.
- [19] Evita, M., Djamal, M., Zimanowski, B. & Schilling, K., *Bandwidth Management for Mobile Mode of Mobile Monitoring System for Indonesian Volcano*, AIP Proceeding of the 6th International Conference on Theoretical and Applied Physics (ICTAP), 2016.
- [20] Evita, M., Zakiyyatuddin, A., Srigutomo, W., Meilano, I. & Djamal, M., *Photogrammetry using Intelligent-Battery UAV in Different Weather for Volcano Early Warning System Application*, Proceeding of the International Conference on Energy Science, submitted for publication.
- [21] Zakiyyatuddin, A., Evita, M., Srigutomo, W., Meilano, I. & Djamal, M., *Geospatial Survey Analysis for 3D Field and Building Mapping using DJI Drone and Intelligent Flight Battery*, Proceeding of the International Conference on Energy Science, submitted for publication.
- [22] Evita, M., Djamal, M., Zimanowski, B. & Schiling, K., *Mobile Robot Deployment Experiment for Mobile Mode of Mobile Monitoring System for Indonesian Volcano*, Proceeding of International Conference on Technology and Social Science, Keynote Lecture, 2017.
- [23] Evita, M., Zakiyyatuddin, A., Seno, S., Kumalasari, R., Lukado, H. & Djamal, M., *Development of a Robust Mobile Robot for Volcano Monitoring Application*, IOP Proceeding of the 9th International Conference on Theoretical and Applied Physics (ICTAP), **1572**, 2019.
- [24] Kayacan, E. & Khanesar, M., A., *Fuzzy Neural Network for Real Time Control Applications*, Elsevier Inc., 2016.
- [25] Noname, G. *Kelud*, Badan Geologi Kementrian Energi dan Sumber Daya Mineral, vsi.esdm.go.id/index.php/gunungapi/data-dasar-gunungapi/538-g-kelud (31 January 2020).
- [26] Noname, *Seismic Monitoring*, Museum Gunungapi Merapi, mgm.slemankab.go.id/pemantauan-seismik/ (31 January 2020).
- [27] Zakaria, N. & Azizah, R., *Analysis of Air Contaminant (SO₂), Throat Irritation and Eyes Irritation of Street Food Vendors around Joyoboyo Bus Station, Surabaya*, The Indonesian Journal of Occupational Safety and Health, **2**(1), pp. 75-81, 2013. (Text in Indonesian and Abstract in English)
- [28] Rice, A.S., *Health Effect of Acute and Prolonged CO₂ Exposure in Normal and Sensitive Populations*, Second Annual Conference on Carbon Sequestration, 2003.
- [29] Arif, M., Arnoraga, B., Handoyo, S. & Nasir, H., *Algorithm Apriori Association Rule in Determination of Fuzzy Rule Based on Comparison of*

- Fuzzy Inference System (FIS) Mamdani Method and Sugeno Method*, Business Management and Strategy, **7**, pp. 103-124, 2016.
- [30] Abbas, A., *Fuzzy Logic Control in Support of Autonomous Navigation of Humanitarian De-mining Robots*, in Using Robots in Hazardous Environments, Baudoin, Y., Habib, M.K. (eds.), Woodhead Publishing Limited, 2011.
- [31] Jang, Y., Peng, L., Hu, A., Wang, S., Huang, Y. & Zhang, L., *Physical Layer Identification of LoRa Devices Using Constellation Trace Figure*, J. Wireless Com Network, **223**, 2019. DOI: 10.1186/s13638-019-1542-x.
- [32] Tsai, K.L., Huang, Y.L., Leu, F.Y., You, I., Huang, Y.L. & Tsai, C.H., *AES-128 Based Secure Low Power Communication for LoRaWAN IoT Environment*, Special Section on Security and Trusted Computing for Industrial Internet of Things, **6**, pp. 45325-45334, 2018.
- [33] Andrei, M.L., Radoi, L.A. & Tudose, D., *Measurement of Node Mobility for the LoRa Protocol*, Proceeding of Networking in Education and Research (RoEduNet), pp. 1-6, 2017.
- [34] Rogers, M.J.B., Hrovat, K., McPherson, K., Moskowitz, M.E. & Reckart, T., *Accelerometer Data Analysis and Presentation Techniques*, NASA, <https://ntrs.nasa.gov/search.jsp?R=19970034695> (31 January 2020)
- [35] Noname, *MPU-6000 and MPU-6050 Product Specification Revision 3.4*, Datasheet4U, datasheet4u.com/datasheet-parts/MPU6050-datasheet.php?id=735134 (31 January 2020).
- [36] Noname, *TGS2602 for the Detection of Air Contaminants*, Figaro, figarosensor.com/product/docs/TGS2602-B00%20%280629.pdf (31 January 2020).
- [37] Noname, *MG811 CO2 Sensor*, Datasheet PDF, datasheetpdf.com/pdf-file/576123/ETC/MG811/1 (31 January 2020).